

A Molecular Dynamics Simulation on the Self-assembly of ABC Triblock Copolymers. 2. Effects of Block Sequence

Min Jae Ko, Seung Hyun Kim, and Won Ho Jo*

Hyperstructured Organic Materials Research Center and School of Materials Science and Engineering,
Seoul National University, Seoul 151-742, Korea

(Received February 26, 2002; Revised March 13, 2002; Accepted March 18, 2002)

Abstract: The effect of block sequence on the self-assembly of ABC-type triblock copolymers in the ordered state is investigated using an isothermal-isobaric molecular dynamics simulation. The block sequence has an important effect on the morphology of ABC triblock copolymers. Different morphologies are observed depending on the block sequence as well as the block composition. The triblock copolymers with the volume fraction of 1:1:1 ($f_A = f_B = f_C = 0.33$) show the three phase and four layered lamellar structures irrespective of the block sequence. The $A_{32}B_{16}C_{32}$ triblock copolymer with $f_B = 0.2$ shows a morphology in which cylinders of midblock B are formed at the interface between A and C lamellae, whereas the morphology of triblock copolymer $B_{16}C_{32}A_{32}$ and $C_{32}A_{32}B_{16}$ show a cylindrical core-shell structure and a lamellar type morphology, respectively. The $A_{20}B_{40}C_{20}$ triblock copolymer with the block B as a major component shows a tricontinuous structure, whereas both $B_{40}C_{20}A_{20}$ and $C_{20}A_{20}B_{40}$ triblock copolymers exhibit the lamellar structures. When the block B has larger volume fraction with $f_B = 0.75$, the matrix is composed of block B, and other two blocks A and C form spherical domains.

Keywords: Molecular dynamics, Self-assembly, ABC triblock copolymer, Block sequence

Introduction

Block copolymers consisting of chemically different blocks undergo microphase separation and show ordered nanoscale structures whose characteristics can be easily controlled by changing the molecular weight, molecular architecture and composition. This microphase separation on a nanoscopic scale is a consequence of the chemical bond between immiscible blocks, which prevent phase separation on a macroscopic scale. Recently, the self-organization of block copolymers in nanoscale has received considerable interest because of their applications in nanotechnology[1-4]. The AB diblock copolymer, the simplest case of block copolymers, is well known to phase-separate into microdomain structures, such as spherical, cylindrical, lamellar and various bicontinuous structures depending on the composition and thermodynamic interaction[5,6].

Introducing block C into an AB diblock copolymer increases the number of possible morphologies due to the large number of independent system variables. This ABC-type triblock copolymers have two independent compositions, three binary interaction parameters, and three different sequences, in comparison to one binary interaction parameter and one composition variable in AB diblock copolymers. Therefore, the microphase separation of triblock copolymers becomes more complicated than for diblock copolymers.

In our previous work[7], we investigated by using a molecular dynamics simulation the effect of block composition on the morphology of symmetric triblock copolymers with both end blocks having equal chain length.

Various structures were observed for ABC triblock copolymers depending upon the block composition. For ABC triblock copolymers with the midblock as a minor component, the structures of the midblock B were changed from lamellar, cylindrical, to spherical morphology at the interface between A/C lamellae as the volume fraction (f_B) of B block decreased. For ABC triblock copolymers with the midblock B as a major component, the morphologies of end blocks were changed from tricontinuous to spherical structures in the matrix composed of midblock as f_B increased.

It is expected that the sequence of three blocks plays an important role in the morphological behavior of triblock copolymers. The sequential order of block in diblock copolymer is meaningless because AB and BA diblock copolymers are indistinguishable. However, the sequential order of three different blocks in triblock copolymer becomes very important since A-B-C, B-C-A, and C-A-B triblock copolymers are distinguishable, as shown in Figure 1. This different sequential order may significantly change the morphology of the triblock copolymers with a given chemical composition, since it affects the thermodynamic conditions between midblock and endblocks. Only few experimental and theoretical studies have addressed the effect of block sequence in triblock copolymers on their morphology. Mogi *et al.*[8] observed a lamellar structure in polyisoprene-polystyrene-poly-2-vinylpyridine (PI-PS-P2VP) triblock copolymers with the volume fraction of 1:1:1, whereas the hexagonally ordered coaxial cylinder phase was found in polystyrene-polysoprene-poly-2-vinylpyridine (PS-PI-P2VP) with the same composition but different sequence by Gido *et al.*[9]. In this system, the interaction between PI

*Corresponding author: whjpoly@plaza.snu.ac.kr

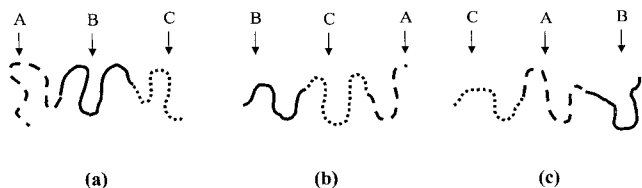


Figure 1. Three different sequences for the ternary linear triblock copolymer: (a) A-B-C type, (b) B-C-A type, (c) C-A-B type triblock copolymers.

and P2VP is much larger as compared to the one between PI and PS. Also, many works on the morphology of PS-PB-PMMA triblock have been accomplished by Stadler and his coworkers[10-13]. According to their report, PS-PB-PMMA exhibits a hexagonally ordered core-shell structure when $\phi_{PS} = 0.64$, $\phi_{PB} = 0.21$, and $\phi_{PMMA} = 0.15$ [12], whereas the change of block sequence into PB-PS-PMMA results in a morphological change from the hexagonally ordered core-shell structure to the cylindrical structure[14,15]. They showed that the interplay between interfacial energies and elastic energies of different block leads to the various morphologies and enhances or prevents mixing of different blocks[15]. Zheng and Wang[16] predicted theoretically that the different sequence in triblock copolymers leads to different morphologies in strong segregation limit. However, a systematic study on the sequence effect of triblock copolymers on the morphology is still lacking, because of the synthesis problems and wide range of the parameter space in ABC triblock copolymers. Under these situations, the computer simulation method would provide a powerful tool to study the morphological behavior of ABC triblock copolymers. Hence, the molecular dynamics (MD) simulation is used in this paper to systematically investigate the effect of block sequence on the morphological structure.

Model and Simulation Method

A detailed description of our model and simulation methods will be found in our previous report[7]. Here, we use the isothermal-isobaric or constant pressure ensemble for MD simulation of ABC triblock copolymers. Although constant pressure simulations are more computationally expensive than canonical simulations, they have some advantages. In a constant volume simulation, the periodicity of microphase separated structures may not match exactly the dimension of the simulation box, especially for small size of system. This means that the structures may not match their preferred shapes in order to be commensurate with the periodic images due to the boundary conditions, leading to a distorted structure of ordered phases. This problem can be avoided by carrying out the constant pressure simulation which allows the shape and volume of simulation box to change.

A coarse-grained generic model is used to simulate the linear ABC type triblock copolymer chain. In this model, each chain is composed of N beads with the identical size. As mentioned above, there are three possible sequences for the linear ABC triblock copolymer. The morphology of triblock copolymer with A-B-C sequence has been discussed in our previous paper[7]. In this work, the copolymers with other sequences, i.e., B-C-A and C-A-B, are simulated and their results are compared with the case of A-B-C, keeping the volume fraction of components fixed. Since only symmetric A-B-C triblock copolymers are considered in our previous paper, the volume fractions of blocks A and C (f_A and f_C) are given by the volume fraction (f_B) of block B as $f_A = f_C = (1 - f_B)/2$ throughout this paper. The chain length of the block B is changed from 16 to 60, while all the triblock copolymers have a constant total chain length of $N = 80$. The total number of chains in the system is 20. Each bead interacts with only two types of potential, E_{vdw} and E_1 . E_{vdw} is a Lennard-Jones (LJ) potential acting between any pair of segments as given by

$$E_{vdw} = 4\epsilon_{ij} \left[\left(\frac{\sigma_{ij}}{r} \right)^{12} - \left(\frac{\sigma_{ij}}{r} \right)^6 - \left(\frac{\sigma_{ij}}{r_c} \right)^{12} + \left(\frac{\sigma_{ij}}{r_c} \right)^6 \right] \quad r \leq r_c \quad (1)$$

where the cut-off distance is set as $r_c = 2^{1/6}\sigma$ to make the potential purely repulsive and r is the distance between the i th and j th segment. The parameters ϵ_{ij} and σ_{ij} are the LJ energy and length parameters for segments i and j , respectively. The length parameters are chosen as $\sigma_{AA} = \sigma_{BB} = \sigma_{CC} = \sigma_{AB} = \sigma_{BC} = \sigma_{CA} = \sigma = 2\text{ \AA}$ so that all types of segments have the same interaction range and the same molar volume. The energy parameters are set as $\epsilon_{AA} = \epsilon_{BB} = \epsilon_{CC} = \epsilon = 1$ kcal/mol, $\epsilon_{AB}/\epsilon = 5$, $\epsilon_{BC}/\epsilon = 10$, and $\epsilon_{CA}/\epsilon = 2$. This set of interaction parameter means that the incompatibility between A and C is smaller than the incompatibility between A and B and between B and C blocks, and the interaction between B and C is the most unfavorable, i.e., $\epsilon_{AC} < \epsilon_{AB} < \epsilon_{BC}$. Here, the energy parameters ϵ_{ij} of this simulation are proportional to the Flory-Huggins interaction parameters χ_{ij} through the relation $\chi_{ij} = z\epsilon_{ij}/k_B T$ where z , k_B , and T are the effective coordination number, the Boltzmann constant and temperature, respectively. Therefore, the ABC triblock copolymer of our simulation with $\epsilon_{AC} < \epsilon_{AB} < \epsilon_{BC}$ corresponds to the PS-PB-PMMA triblock copolymer with $\chi_{PS-PMMA} < \chi_{PS-PB} < \chi_{PB-PMMA}$ [10-13]. E_1 is bond stretching potential along the chains, as given by

$$E_1 = \frac{1}{2} k_b (l - l_0)^2 \quad (2)$$

where k_b is the energy parameter of the potential, l is the distance between two neighboring segments of the same chain, and l_0 is a length parameter at which the potential has a minimum value. We have chosen $k_b = 10^3 \epsilon/\sigma^2$ and $l_0 = 0.75\sigma$ to avoid the bond crossing[17]. The time scale in this model is given by $\tau = \sigma(m/\epsilon)^{1/2}$, where m is the mass of a

segment.

In this study, all simulations are performed on the commercial modeling software, *Cerius*² of Molecular Simulations Inc. The initial configurations are randomly generated in a cubic cell with the dimensions of $25 \sigma \times 25 \sigma \times 25 \sigma$ and then energy-minimized. Before implementing the isothermal-isobaric dynamics, the systems are fully relaxed by the canonical ensemble molecular dynamics. The initial number density of triblock copolymers is set as $\rho = 0.85 \sigma^{-3}$, and the temperature is set as $T = \epsilon/k_B = 1.0$. The pressure obtained from NVT simulation is used as an external pressure in the following NPT simulation. Through the NPT molecular dynamics under $P = 25 \epsilon/\sigma^3$ for $5 \times 10^4 \tau$ with the time step of $\Delta t = 0.01 \tau$, final equilibrium morphologies are obtained.

Results and Discussion

The simulation results for symmetric ABC triblock copolymers with various compositions are reported in our previous paper[7]. In the present work, the morphology of triblock copolymers with different sequential order (B-C-A and C-A-B) is simulated and compared with the A-B-C case. Figure 2 compares the three cases having different sequential order. As expected, the morphology of $A_{27}B_{26}C_{27}$ with $f_A = f_B = f_C = 0.33$, where the number in subscript of each block notation indicates the chain length of each block, shows the lamellar morphology. When the block sequence is changed to B-C-A ($B_{26}C_{27}A_{27}$) and C-A-B ($C_{27}A_{27}B_{26}$), the three-phase and four-layered lamellar structures are also observed. To further identify the lamellar structures, the collective structure factor $S(q)$ is calculated by using the following relation:

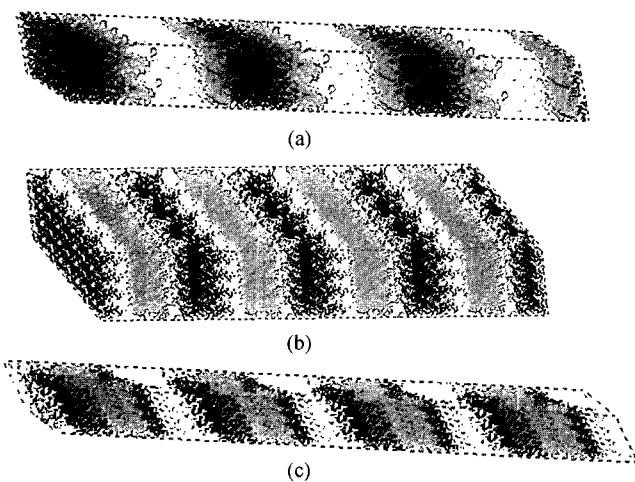


Figure 2. Snapshot of triblock copolymers with $f_A = f_B = f_C = 0.33$ after $5 \times 10^4 \tau$: (a) $A_{27}B_{26}C_{27}$, (b) $B_{26}C_{27}A_{27}$, (c) $C_{27}A_{27}B_{26}$, where A, B and C segments are colored black, gray and white, respectively.

$$S(q) = \left\langle \sum_{ij} \exp(i\mathbf{q} \cdot \mathbf{r}_{ij}) \psi(r_i) \psi(r_j) \right\rangle \quad (3)$$

where \mathbf{q} is the scattering vector, \mathbf{r}_{ij} is the distance vector between segments i and j , the occupation factor $\psi(r_i)\psi(r_j) = 1$ for the same segments and -1 for unlike segments. When the calculated $S(q)$ is plotted against q in Figure 3, characteristic Bragg-peaks of higher order are observed at the integer multiples of q^* , indicating that the three block copolymers form the lamellar structure. As shown in Figure 2, the lamellae formed from both end blocks are almost two times as thick as midblock lamellae, since the lamellae are arranged sequentially in a way of [ABCCBA], [BCAACB], and [CABBAC] for A-B-C, B-C-A, and C-A-B triblock

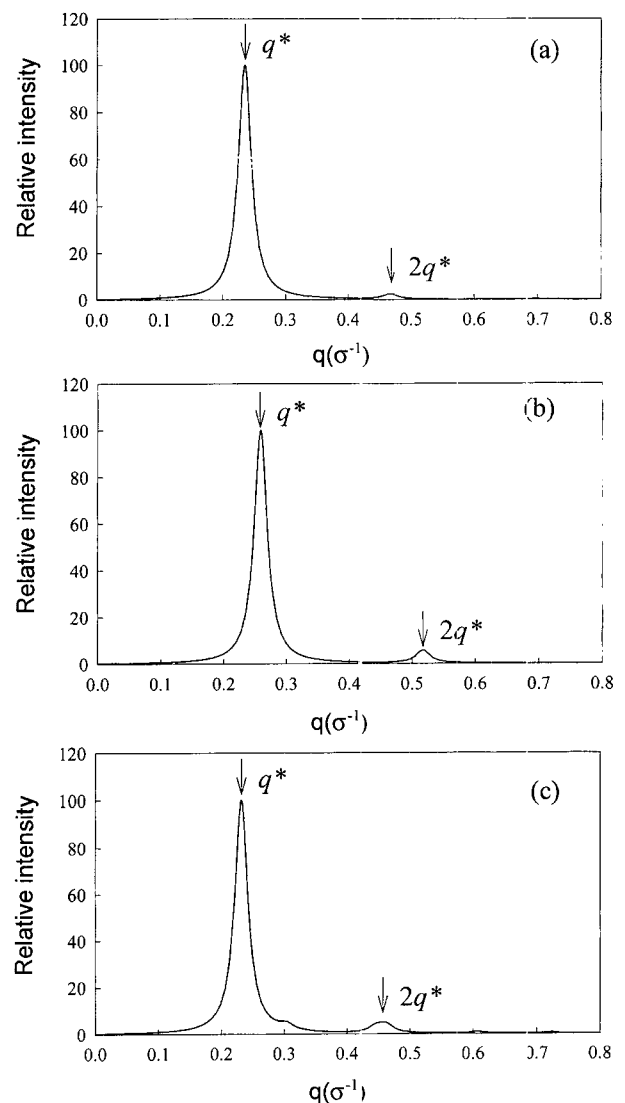


Figure 3. Simulated scattering pattern of (a) $A_{27}B_{26}C_{27}$, (b) $B_{26}C_{27}A_{27}$ and (c) $C_{27}A_{27}B_{26}$ triblocks after $5 \times 10^4 \tau$, where the intensity of peaks is normalized with respect to that of the first order peak.

copolymers, respectively. Zheng and Wang[16] predicted the similar morphologies in the phase diagram of PS-PEB-PMMA at the same composition under similar thermodynamic condition.

In the case of $A_{32}B_{16}C_{32}$ with $f_B = 0.2$, cylinders of midblock B are formed at the interface between A and C lamellae, as reported in our previous paper[7]. The effects of block sequence on the morphology at this block composition are shown in Figure 4. The snapshot of triblock copolymer $B_{16}C_{32}A_{32}$ shows that a cylindrical core-shell morphology in which a B cylinder is surrounded by a C cylindrical shell is formed in the A matrix. This morphology is similar to the "cylinder in cylinder" morphology as previously reported for SBM triblock copolymers[12]. This morphology results from two different repulsive interactions between the middle and the two end blocks as compared to ABC in conjunction with the smaller volume fraction of block B. In other words, since the incompatibility between B and C is larger than that between C and A, the system tends to form a smaller interface between B and C than that between C and A. Considering the connectivity between the block B and the middle block C, the formation of interface between B and C is unavoidable. As a consequence, the block C may form the shell around the core cylinder composed of block B. The morphology developed from $C_{32}A_{32}B_{16}$ triblock exhibits a different structure from the $A_{32}B_{16}C_{32}$ and $B_{16}C_{32}A_{32}$ triblocks, as shown in Figure 4c. The overall morphology of $C_{32}A_{32}B_{16}$ is lamellar, but the microdomain of block B becomes cylinder in shape due to the shorter chain length of endblock B. In other words, the cylinders of B block are embedded in the A lamellae while C block forms the other lamellae. As mentioned above, the interaction between B and C is more repulsive than that between A and B, and therefore this suppresses the direct contact between B and C components, leading to the inclusion of B cylinder into A lamellar microdomain. Here, it is noted that the block B is not directly connected to the block C contrary to the case of $B_{16}C_{32}A_{32}$ triblock. Similar morphology was experimentally observed by Abetz and Goldacker[18] in a mixture of 70% PS-PB-PMMA and 30% PB-PS-PMMA, in which a basic structural unit consists of four layers, and PB cylinders are formed in PS lamellae.

The sequence change of the $A_{20}B_{40}C_{20}$ triblock copolymer with $f_B = 0.5$ may yield different morphologies. The $A_{20}B_{40}C_{20}$ triblock copolymer showed a tricontinuous structure in our previous report, while the $B_{40}C_{20}A_{20}$ and $C_{20}A_{20}B_{40}$ triblock copolymers show different morphologies, i.e., three-phase and four-layered lamellae structures, as shown in Figure 5. For $B_{40}C_{20}A_{20}$, the layers must be formed by the "BCAACB" stacking mode, since the block sequence is [BCA]. Hence, the ratio of lamellar thickness becomes 4:1:2 for B, C, and A lamellae, respectively. The same behavior is observed for the $C_{20}A_{20}B_{40}$ triblock copolymer, where the ratio of lamellar thickness is 4:1:2 for B, A, and C

lamellae, respectively.

Finally, the sequence effect is examined on triblock copolymers with a larger volume fraction of B block, i.e., the result for $A_{10}B_{60}C_{10}$ with $f_B = 0.75$ is compared with those for $B_{60}C_{10}A_{10}$ and $C_{10}A_{10}B_{60}$. As discussed in our previous paper[7], two end blocks form one spherical domain, as shown in Figure 6a. The possibility of mixing of A and C blocks in one spherical domain was also predicted in theoretical calculation by Stadler and his coworkers[19,20]. When the block sequence is changed to B-C-A ($B_{60}C_{10}A_{10}$), a similar morphology is observed, as shown in Figure 6b. The block B forms the matrix due to the larger volume fraction with respect to A and C blocks, while the A and C blocks seem to form one spherical domain, as in the case of $A_{10}B_{60}C_{10}$ triblock. However, a closer examination reveals that the midblock C is located at the phase boundary between spheres and matrix. This is because the midblock C is connected with the both end blocks. In other words, since two end blocks A and B form the dispersed phase and matrix, respectively, it is most probable that the midblock C is located at the interface between A and B domains. This explanation is also applicable to the C-A-B ($C_{10}A_{10}B_{60}$) case, where the block A is located at the interface between the matrix B and the dispersed phase C, as shown in Figure 6. Recently, Breiner *et al.*[13] observed a similar morphology in the asymmetric ABC triblock copolymer with small volume fraction of midblock and one of endblocks. They designated this morphology as the "spheres on sphere" structure.

Conclusions

We investigated the effect of block sequence on the self-assembly of ABC triblock copolymers using a molecular dynamics simulation. In our previous work, we thoroughly investigated the effect of block composition on morphology of the symmetric A-B-C triblock copolymers in which the volume fraction of A and C is the same, i.e., $f_A = f_C$. In this work, when the block sequence A-B-C is changed to B-C-A or to C-A-B, the different self-assembling behavior of triblock copolymers is observed. When each of three components in triblock copolymers has an equal composition, three-phase and four-layered lamellar structures are observed for A-B-C ($A_{27}B_{26}C_{27}$), B-C-A ($B_{26}C_{27}A_{27}$) and C-A-B ($C_{27}A_{27}B_{26}$). When the block composition is changed to $A_{32}B_{16}C_{32}$ with $f_B = 0.2$, cylinders of midblock B are formed at the interface between A and C lamellae. Changing the block sequence at this block composition from ABC to BCA or to CAB results in the change of morphology, i.e., the morphology of triblock copolymers $B_{16}C_{32}A_{32}$ and $C_{32}A_{32}B_{16}$ show a cylindrical core-shell structure and a lamellar type morphology, respectively. For the triblock copolymers with block B as a major component, $A_{20}B_{40}C_{20}$ shows a tricontinuous structure, whereas both $B_{40}C_{20}A_{20}$ and

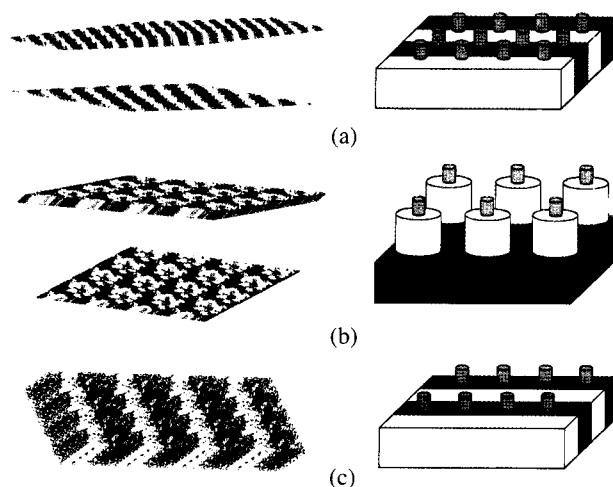


Figure 4. Snapshot of triblock copolymers with $f_A = f_C = 0.4$ and $f_B = 0.2$ after $5 \times 10^4 \tau$: (a) $A_{32}B_{16}C_{32}$, (b) $B_{16}C_{32}A_{32}$, (c) $C_{32}A_{32}B_{16}$, where A, B and C segments are colored black, red and yellow, respectively. Schematic representations of each morphological structure are shown in the right side. The top views of $A_{32}B_{16}C_{32}$ and $B_{16}C_{32}A_{32}$ are also shown in the lower left side of each figure. The cylinders of B blocks in $A_{32}B_{16}C_{32}$, $B_{16}C_{32}A_{32}$ and $C_{32}A_{32}B_{16}$ are located at the interface of lamellae, in the C cylinders, and in the A lamellae, respectively.

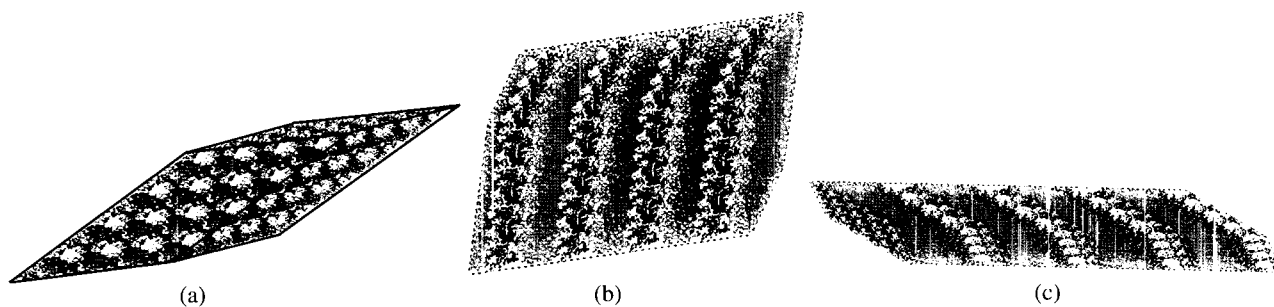


Figure 5. Snapshot of triblock copolymers with $f_A = f_C = 0.25$ and $f_B = 0.5$ after $5 \times 10^4 \tau$: (a) $A_{20}B_{40}C_{20}$; (b) $B_{40}C_{20}A_{20}$; (c) $C_{20}A_{20}B_{40}$, where A, B and C segments are colored black, red and yellow, respectively.

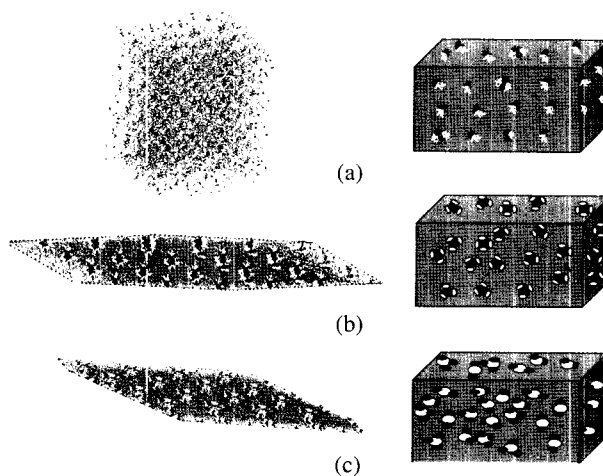


Figure 6. Snapshot of triblock copolymers with $f_A = f_C = 0.125$ and $f_B = 0.75$ after $5 \times 10^4 \tau$: (a) $A_{10}B_{60}C_{10}$; (b) $B_{60}C_{10}A_{10}$; (c) $C_{10}A_{10}B_{60}$, where A, B and C segments are colored black, red and yellow, respectively. Schematic representations of each morphological structure are shown in the right side.

$C_{20}A_{20}B_{40}$ triblock copolymers exhibit the lamellar structures. When the block B has larger volume fraction with $f_B = 0.75$, the matrix is composed of the block B, and other two blocks A and C form spherical morphologies.

In summary, it can be concluded from our simulation results that both the block sequence and the block composition of ABC block copolymers plays a decisive role in determining the morphology of the triblock copolymers, since they can affect the thermodynamic conditions between midblock and endblocks. Considering that it is not always possible to examine experimentally the block sequence effect of ABC triblock copolymers on their morphology, the computer simulation provides a powerful tool to predict the morphology when the block composition and thermodynamic condition of components are given.

Acknowledgement

The authors thank the Korea Science and Engineering Foundation (KOSEF) for their financial support through the Hyperstructured Organic Materials Research Center (HOMRC).

References

1. M. Park, C. Harrison, P. M. Chaikin, R. A. Register, and D. H. Adamson, *Science*, **276**, 1401 (1997).
2. S. E. Webber, P. Munk, and Z. Tuzar, "Solvents and Self-Organization of Polymers", Kluwer Academic Publishers, Dordrecht, 1996.
3. I. W. Hamley, "The Physics of Block Copolymers", Oxford University Press, London, 1998.
4. T. Okano, "Biorelated Polymers and Gels: Controlled Release and Applications in Biomedical Engineering", Academic Press, San Diego, 1998.
5. L. Leibler, *Macromolecules*, **13**, 1602 (1980).
6. G. H. Fredrickson and F. S. Bates, *Annu. Rev. Phys. Chem.*, **41**, 525 (1990).
7. M. J. Ko, S. H. Kim, and W. H. Jo, *Macromol. Theory Simul.*, **10**, 381 (2001).
8. Y. Mogi, M. Nomura, H. Kotsuji, K. Ohnishi, Y. Matsushita, and I. Noda, *Macromolecules*, **27**, 6755 (1994).
9. S. P. Gido, D. W. Schwark, E. L. Thomas, and M. D. Goncalves, *Macromolecules*, **26**, 2636 (1993).
10. C. Auschra and R. Stadler, *Macromolecules*, **26**, 2171 (1993).
11. R. Stadler, C. Auschra, J. Beckmann, U. Krappe, I. Voigt-Martin, and L. Leibler, *Macromolecules*, **28**, 3080 (1995).
12. U. Breiner, U. Krappe, V. Abetz, and R. Stadler, *Macromol. Chem. Phys.*, **198**, 1051 (1997).
13. U. Breiner, U. Krappe, T. Jakob, V. Abetz, and R. Stadler, *Polym. Bull.*, **40**, 219 (1998).
14. K. Jung, A. Volker, and R. Stadler, *Macromolecules*, **29**, 1076 (1996).
15. V. Abetz and R. Stadler, *Macromol. Symp.*, **113**, 19 (1997).
16. W. Zheng and Z. Wang, *Macromolecules*, **28**, 7215 (1995).
17. K. Binder, "Monte Carlo and Molecular Dynamics Simulations in Polymer Science", Oxford University Press, New York, 1995.
18. V. Abetz and T. Goldacker, *Macromol. Rapid Commun.*, **21**, 16 (2000).
19. V. Abetz, R. Stadler, and L. Leibler, *Polym. Bull.*, **37**, 135 (1996).
20. I. Erukhimovich, V. Abetz, and R. Stadler, *Macromolecules*, **30**, 7435 (1997).